Received: 6 July 2023 | Revised: 10 October 2023 | Accepted: 22 October 2023

DOI: 10.1002/bit.28589

ARTICLE

BIOTECHNOLOGY AND BIOENGINEERING WILEY

Co-current filtrate flow in TFF perfusion processes: Decoupling transmembrane pressure from crossflow to improve product sieving

Patrick Romann[1,2] | Philip Giller[1] | Antony Sibilia[3] | Christoph Herwig[2] | Andrew L. Zydney[4] | Arnaud Perilleux[5] | Jonathan Souquet[5] | Jean-Marc Bielser[5] | Thomas K. Villiger[1]

[1]School of Life Science, Institute for Pharma Technology, University of Applied Sciences and Arts Northwestern Switzerland, Muttenz, Switzerland

[2]Research Division Biochemical Engineering, Institute of Chemical Environmental and Bioscience Engineering, Vienna University of Technology, Vienna, Austria

[3]Levitronix GmbH, Zürich, Switzerland

[4]Department of Chemical Engineering, The Pennsylvania State University, University Park, Pennsylvania, USA

[5]Biotech Process Science, Merck Serono SA (an affiliate of Merck KGaA, Darmstadt, Germany), Corsier-sur-Vevey, Switzerland

Correspondence
Thomas K. Villiger
Email: thomas.villiger@fhnw.ch

Abstract

Hollow fiber-based membrane filtration has emerged as the dominant technology for cell retention in perfusion processes yet significant challenges in alleviating filter fouling remain unsolved. In this work, the benefits of co-current filtrate flow applied to a tangential flow filtration (TFF) module to reduce or even completely remove Starling recirculation caused by the axial pressure drop within the module was studied by pressure characterization experiments and perfusion cell culture runs. Additionally, a novel concept to achieve alternating Starling flow within unidirectional TFF was investigated. Pressure profiles demonstrated that precise flow control can be achieved with both lab-scale and manufacturing-scale filters. TFF systems with co-current flow showed up to 40% higher product sieving compared to standard TFF. The decoupling of transmembrane pressure from crossflow velocity and filter characteristics in co-current TFF alleviates common challenges for hollow fiber-based systems such as limited crossflow rates and relatively short filter module lengths, both of which are currently used to avoid extensive pressure drop along the filtration module. Therefore, co-current filtrate flow in unidirectional TFF systems represents an interesting and scalable alternative to standard TFF or alternating TFF operation with additional possibilities to control Starling recirculation flow.

KEYWORDS

co-current filtrate flow, perfusion cell culture, product sieving, Starling recirculation, tangential flow filtration (TFF)

Abbreviations: ATF, alternating tangential flow filtration; CD_F, centrifugal discharge pump in filtrate loop; CD_{R1-2}, centrifugal discharge pump in retentate loop; fs_f, flow sensor in filtrate loop; FS_R, flow sensor in retentate loop; HPTFF, high-performance tangential flow filtration; PP_H, peristaltic pump in harvest line; PT_{A1-5}, additional pressure transmitter on filtrate side of hollow fiber filter; PT_{AB1-5}, additional pressure transmitter on backside of filtrate side of hollow fiber filter; PT_{F1-2}, pressure transmitter in filtrate loop; PT_{R1-2}, pressure transmitter in retentate loop; rTFF, reverse tangential flow filtration; scTFF, stepping co-current tangential flow filtration; TFF, tangential flow filtration; TMP, transmembrane pressure; VCD, viable cell density; VCV, viable cell volume.

1 | INTRODUCTION

Hollow fiber-based tangential flow filtration (TFF) has emerged as one of the most preferred cell retention technologies for mammalian perfusion processes with applications in main-stage perfusion bioreactors and also in *N*−1 bioreactors to improve existing fed-batch production units (Bielser et al., 2018; Coffman et al., 2021; Wolf et al., 2020). Despite significant advancements in pump technology, such as low-shear diaphragm pumps or levitated centrifugal pumps (Blaschczok et al., 2013; Clincke et al., 2013; Kelly et al., 2014; Wang et al., 2017), to improve culture viability and thereby reduce the load of fouling-provoking particles on the filter membrane, filter clogging and product retention remain major challenges on the way to robust manufacturing processes.

TFF in unidirectional crossflow mode (frequently driven by a levitated centrifugal pump) and alternating tangential flow (ATF, driven by a diaphragm pump) are the most commonly reported systems in perfusion processes (Fisher et al., 2019; MacDonald et al., 2022; Matanguihan & Wu, 2022). Most studies revealed that ATF showed superior product sieving compared to TFF at lab-scale and suggested ATF as a more suitable technology for long-term perfusion operation (Clincke et al., 2013; Karst et al., 2016; Wang et al., 2017). However, ATF systems driven by diaphragm pumps were associated with operational instability at the manufacturing scale (Coffman et al., 2021; Pavlik, 2017, 2019; Shevitz, 2018). Furthermore, multiple parallel ATF systems were required to operate 2000 L perfusion bioreactors, requiring considerably more floor space compared to similar TFF systems (Coffman et al., 2021; Romann et al., 2023). Therefore, TFF systems were claimed to be the preferred choice within the industry at large scale due to smaller facility footprint and higher robustness, whereas ATF systems showed improved product sieving and reduced development time for pilot-scale operations (Coffman et al., 2021).

In TFF, concentration polarization and fouling can both affect product retention (Belfort et al., 1994; Chew et al., 2020; Field, 2010; Taddei et al., 1990; van Reis & Zydney, 2007). Compared to industrial TFF applications that have short operating times and high filtrate flux (Redkar & Davis, 1993; Tanaka et al., 1997; Weinberger & Kulozik, 2021b), TFF systems used as cell retention devices in perfusion processes must be operational for as much as several months (without cleaning) and are operated at comparably very low filtrate fluxes of around 2 L/m^2/h (Radoniqi et al., 2018). Due to the low filtrate fluxes and high axial pressure drops, a reverse flow of filtrate back into the fiber lumen occurs at the filter exit. This so-called Starling recirculation (Starling, 1896) was modeled and shown to be significantly larger than the actual harvest rate during typical perfusion processes (Radoniqi et al., 2018). As a consequence, only slightly more than 50% of the actual hollow fiber membrane surface area is used for filtration (Radoniqi et al., 2018).

More recently, alternating TFF systems have been described either with one levitated centrifugal pump and valves to switch crossflow direction (Weinberger & Kulozik, 2021a), or with two alternating, inversely positioned centrifugal pumps in the retentate loop called reverse TFF (rTFF) (Pappenreiter et al., 2023; Weinberger & Kulozik, 2022). Both setups showed reduced product retention compared to unidirectional TFF systems. While each individual phase of alternating crossflow filtration (ATF, rTFF, or alternating crossflow by valve switching) can be compared to the situation in a TFF system, the distinguishing factor lies in the alternating direction of the crossflow and therefore the change in the location of the filter inlet. When working with cell lines prone to aggregation, switching the filter inlet can prevent fiber blocking (Weinberger & Kulozik, 2021a; Zydney, 2016). Improved product sieving with alternating crossflow systems compared to TFF was further attributed to the short period of zero net flow between phases resulting in a very low transmembrane pressure (TMP) across the entire filter length, possibly leading to deposit layer relaxation (Weinberger & Kulozik, 2021a, 2021b). It was also suggested that the Starling recirculation, which switches between the two ends of the hollow fiber, could remove deposited material and thereby minimize fouling (Karst et al., 2016; Radoniqi et al., 2018). Additionally, alternating crossflow filtration makes use of the entire filter length, harnessing the full membrane surface of the module (Radoniqi et al., 2018). The increased performance of alternating TFF is likely due to a combination of these factors.

Although there are several advantages associated with alternating crossflow filtration, it is important to note that the backflush of filtrate at the filter exit must be counterbalanced by an increased filtrate flux near the filter inlet to maintain the same overall level of filtration. This causes an increase in the drag forces that push particles into the membrane (Ripperger & Altmann, 2002), which can lead to a denser deposit and greater particle penetration into the membrane, both detectable as an increase of irreversible fouling resistance (Weinberger & Kulozik, 2022). Sundar et al. (2023) demonstrated that the greatest fouling in ATF systems occurs at the ends of the hollow fiber module, that is, where the filtrate flux is greatest. This might explain studies observing significant product sieving losses despite using properly sized ATF modules (Kim et al., 2016; Wang et al., 2017).

These phenomena provide notable constraints in hollow fiber designs and determining optimal operating conditions for perfusion systems. Crossflow velocities, for example, must be kept low to decrease the pressure drop along the filter length and thereby reduce the Starling recirculation. However, reducing crossflow increases the residence time of the cells within the recirculation loop, risking oxygen depletion (Walther et al., 2019). In addition, low crossflow leads to greater concentration polarization, that is, greater accumulation of cells at the membrane surface. The increasing axial pressure drop with increasing length of the hollow fiber modules favors the use of relatively short filtration modules, requiring multiple filters in parallel to meet the needs for larger filtration area. Increasing the inner diameter of the hollow fibers would also reduce the pressure drop along the fiber length, but at a cost of much greater hold-up volume within the module.

Although all these strategies to improve filtration performance try to reduce the impact of the pressure drop and Starling flow, none of them solve the fundamental problem that the local TMP is coupled

to the magnitude of the crossflow (which determines the axial pressure drop) and the filter characteristics. To achieve a nearly uniform TMP throughout the module, a similar pressure drop must be generated on the filtrate side of the module as on the retentate side. This concept for the biopharmaceutical industry was originally called high-performance TFF (HPTFF) and was successfully demonstrated to control concentration polarization along the filter length to enable high-resolution protein–protein separations in downstream operations (van Reis, 1993; van Reis et al., 1997). It has also improved the purification of viral vectors using ultrafiltration (Grzenia et al., 2008). The concept is further known in the dairy industry for microfiltration (Merin & Daufin, 1990; Sandblom, 1978; Vadi & Rizvi, 2001). The ability to control the filtrate flux and Starling flow independently of the crossflow and length of the filtration module offers a promising tool to overcome challenges in current TFF and ATF systems in perfusion processes. To the authors' knowledge, HPTFF to alleviate product retention in perfusion processes has not been evaluated in the literature.

The aim of this study was to develop a co-current filtration flow system for perfusion processes based on single-use low-shear centrifugal pumps in combination with pressure sensors with the ultimate goal to reduce product retention. This so-called HPTFF system was characterized for a wide range of operating conditions by measuring the TMP along the length of the filter module. Steady-state perfusion cell culture runs demonstrated superior performance during HPTFF compared to standard TFF. Further, a new concept of stepping co-current TFF (scTFF) was introduced, allowing us to generate alternating Starling recirculation within a unidirectional TFF system. Subsequently, the scalability of HPTFF and scTFF were successfully evaluated by recording pressure profiles along a modified large-scale hollow fiber module.

2 | MATERIALS AND METHODS

2.1 | Lab-scale system setup for pressure characterization

An experimental setup capable of operating TFF, rTFF, HPTFF, and scTFF was built to characterize the different filtration systems at lab-scale (Figure 1a). Pressure transmitters (PREPS-N-038, PendoTECH) were installed in the retentate loop at the inlet (PT_{R1}) and outlet of the filter (PT_{R2}). Further pressure transmitters were positioned in the filtrate loop at the inlet (PT_{F1}) and outlet (PT_{F2}) of the module. A PES hollow fiber module with a total module length of 70 cm, an effective fiber length of 65 cm, an inner fiber diameter of 1 mm, a pore size of 0.2 µm, and a membrane surface area of 0.15 m^2 was used (S06-P20U-10-N; Repligen). For the pressure tests, the hollow fiber module was modified by drilling holes and gluing additional pressure transmitters (PT_{A1-5}) into the filtrate side to monitor the filtrate pressures along the filter length. Considering the total length of the hollow fiber module, the additional pressure transmitters (PT_{A1-5}) were place at 5.5, 20, 35, 50, and 64.5 cm measured from the start of the module. Flow sensors (LFSC-i10X-001; Levitronix GmbH) were installed in the retentate loop (FS_R) and in the filtrate loop (FS_F). Three levitated centrifugal pumps (PuraLev i30SU; Levitronix GmbH) were integrated into the experimental setup. Two pumps were integrated into the retentate loop, of which one was directed toward the filter inlet (CD_{R1}) and the other toward the filter outlet (CD_{R2}). The third centrifugal pump (CD_F) was inserted into the filtrate loop directed toward the filter inlet side. A peristaltic pump (PP_H) was inserted into the harvest stream. Data were recorded by connecting three process control units (LCO-i100; Levitronix GmbH).

2.2 | Large-scale system setup for pressure characterization

For large-scale pressure characterization, a similar experimental setup as described for lab-scale experiments was built to achieve TFF, HPTFF, and scTFF operation (Figure 7a,b). A PES hollow fiber module with a total module length of 78 cm, an effective fiber length of 68 cm, an inner fiber diameter of 1 mm, a pore size of 0.2 µm, and a membrane surface of 7.15 m^2 was used (X06-P20U-10-N; Repligen). Pressure transmitters (PREPS-N-1-1; PendoTECH) were installed in the retentate loop (PT_{R1}) and PT_{R2}) and in the filtrate loop (PT_{F1} and PT_{F2}). To measure pressures as closely as possible to the inlet and outlet of the hollow fibers, holes were drilled to place pressure transmitters (PREPS-N-038' PendoTECH) into the adapter piece of the filter module (PT_{RC1} and PT_{RC2}). Further pressure transmitters (PREPS-N-038; PendoTECH) on the filtrate side were attached along the filter length at 15.5, 27.5, 38.5, 50, and 62.5 cm measured from the start of the module (PT_{A1-5}). Additionally, pressure transmitters at the same filter length but in the back were attached (PT_{AB1-5}). Flow sensors (LFSC-i35X; Levitronix GmbH) were installed in the retentate (FS_R) and filtrate loops (FS_F). One levitated centrifugal pump (PuraLev-2000SU; Levitronix GmbH) was inserted into the retentate loop (CD_{R1}) and a second levitated centrifugal pump (PuraLev-600SU; Levitronix GmbH) was placed in the filtrate loop (CD_F). A peristaltic pump (PP_H) was inserted into the harvest stream. Data recording were achieved by coupling six process control units (5× LCO-i100 and 1× LCO-600; Levitronix GmbH).

2.3 | Experimental procedure for pressure characterization

Pressure characterization studies were performed with water as a medium. To characterize the TFF system, only pump CD_{R1} was operational. To realize the HPTFF and scTFF systems, pump CD_{R1} in the retentate loop and pump CD_F in the filtrate loop were active simultaneously. For the rTFF systems, pump CD_{R1} was used for the first phase and pump CD_{R2} was used for the second phase with reversed crossflow. For all lab-scale setups, crossflow was kept at 650 mL/min, except for ramping experiments where the crossflow was ramped from 0 to 1500 mL/min. For crossflow ramping in

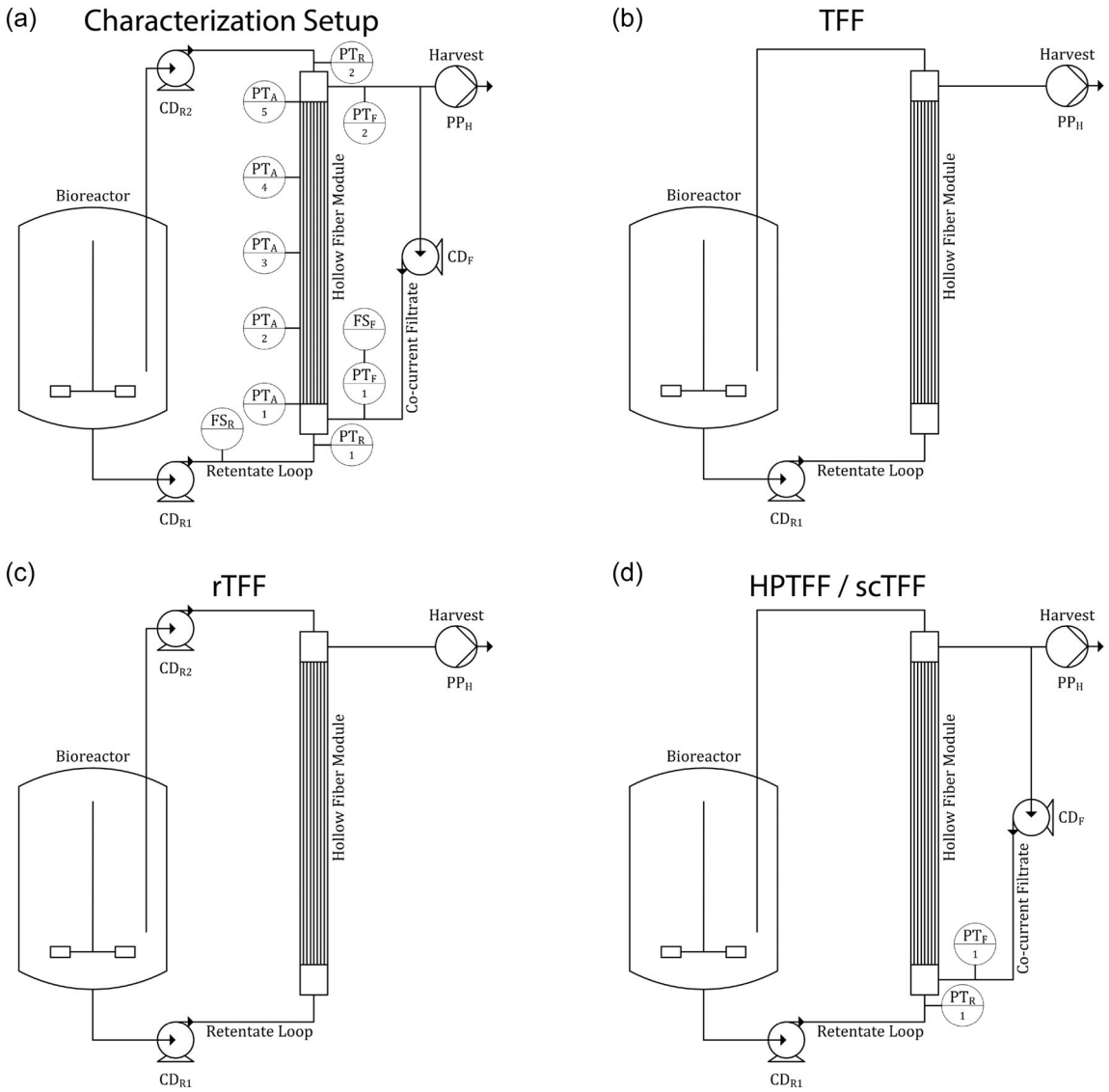

FIGURE 1 Detailed schematic representation of the experimental setup for the pressure characterization in water (a). Pressure transmitters (PT), flow sensors (FS), centrifugal pumps (CD) and peristaltic pumps (PP) are specified with subscripted letters according to their position (A, additional sensors on filtrate side; F, filtrate; H, harvest; R, retentate). Minimal required setups for tangential flow filtration (TFF) (b), reverse TFF (rTFF) (c), and high-performance TFF (HPTFF) or stepping co-current TFF (scTFF) (d) operation used for cell culture runs are further shown.

HPTFF, a delta pressure proportional-integral control (P-term: 2 rpm/Δmbar; I-term: 5 rpm/Δmbar × s) was used with a setpoint of 0 mbar, meaning that the pump speed of pump (CD_F) was controlled such that pressure PT_{F1} matched PT_{R1}. For scTFF characterization, the co-current filtrate flow rate was set at 870 mL/min (scTFF phase 1) and 1890 mL/min (scTFF phase 2) to achieve a delta pressure control of ±10 mbar. To characterize large-scale TFF operation, the crossflow was ramped from 0 to 45 L/min. For HPTFF pressure characterization, additional filtrate flow was applied by a delta pressure proportional-integral control (P-term: 2 rpm/Δmbar; I-term: 5 rpm/Δmbar × s) such that PT_{F1} was kept 6 mbar higher than PT_{R1}. Filtrate flow ramping to assess scTFF operation was achieved by maintaining a crossflow of 14.5 L/min and ramping the co-current filtrate flow from 0 to 70 L/min. To compare filtration conditions between filtration module scales, shear rates provided by the manufacturers' lookup tool were considered (Repligen).

2.4 | Perfusion culture process

A proprietary CHO-K1 cell line producing a bispecific mAb was expanded in an incubator (Multitron, Infors HT) for 21 days using a proprietary chemically defined perfusion platform medium and an on-demand proprietary feed (Merck KGaA). Perfusion bioreactors (Labfors 5 Cell, Infors HT) were inoculated at a seeding density of 0.6×10^6 viable cells/mL. Culture conditions were maintained at 36.5°C with a dissolved oxygen setpoint at 50% (VisiFerm DO Arc, Hamilton). The pH was controlled at 7.07 ± 0.17 (EasyFerm

Plus Arc probe Hamilton) by sparging CO_2 and using a 1.1 M Na_2CO_3 solution. Bioreactors were operated at 2 L working volume. After an initial growth phase, an online capacitance probe (Incyte Arc, Hamilton) was used to keep the viable cell volume (VCV) constant at 12%. Perfusion started on Day 0 and was kept constant at 1.3 reactor volumes per day until the end of the process.

2.5 | Cell retention devices in perfusion cell culture

Bioreactor harvests were gravimetrically controlled to maintain the bioreactor weight constant using the same hollow fiber module as described in Section 2.1. Cell retention devices were either operated as TFF (Figure 1b), rTFF (Figure 1c), HPTFF, or scTFF systems (Figure 1d). Perfusion runs in duplicates were performed for TFF (TFF_1 and TFF_2), for rTFF (rTFF_1 and rTFF_2), and for HPTFF (HPTFF_1 and HPTFF_2). For scTFF, a single perfusion run was performed (scTFF_1). A new hollow fiber module was used for each perfusion run. In all setups, the crossflow was generated by levitated centrifugal pumps (PuraLev i30SU; Levitronix GmbH) to ensure comparability of sieving studies. Pump speeds in the retentate loop were set to 3500 rpm, initially corresponding to a crossflow velocity of 650 mL/min. For TFF, HPTFF, and scTFF operations, the retentate loop pump (CD_{R1}) was stopped every 3 min for 3 s to release accumulated air bubbles within the centrifugal pump head. For HPTFF operations, a delta pressure proportional-integral control (P-term: 2 rpm/Δmbar; I-term: 5 rpm/Δmbar × s) between pressure PT_{R1} and pressure PT_{F1} was used with a setpoint of 0 mbar to control the speed of the filtrate pump (CD_F). As such, filtrate pressures were matched with retentate pressures along the filter length. scTFF operation was achieved by delta pressure control of −5 mbar during scTFF phase 1 and +5 mbar during scTFF phase 2 between pressure PT_{R1} and pressure PT_{F1}. rTFF operation consisted of two phases. In the first phase, the first retentate pump (CD_{R1}) was operational and the second retentate pump (CD_{R2}) was stopped. During the second phase, pump (CD_{R2}) was operational and the pump (CD_{R1}) was stopped. Phase times were 20 s.

2.6 | Reference analytics

Cell density, viability, cell diameter, and pH were measured using a BioProfile FLEX2 (Nova Biomedical). Bioreactors were automatically sampled by the FLEX2 On-Line Autosampler (Nova Biomedical) and samples were fractionated using a Teledyne Cetac ASX-7200 (Teledyne CETAC Technologies). VCV was calculated as follows (Metze et al., 2020):

$$VCV = \frac{4}{3}\cdot\pi\cdot\left(\frac{D}{2}\right)^3 \cdot VCD \cdot 100 \quad (1)$$

where D is the average cell diameter and VCD is the viable cell density, assuming a spherical shape of the cells. Bioreactor samples, taken directly from the bioreactor, were prepared by centrifugation (3200g for 10 min). Cell debris was measured in the supernatant after centrifugation using an optical density (OD) measurement at 600 nm against a 0.22 µm filtered reference sample (Spectronic Genesys 10 Bio; Thermo Electron Corporation). Bioreactor titer (from the collected supernatant) and harvest titer were determined using a protein A affinity high-performance liquid chromatography device (PA-HPLC; Waters). Consequently, the ratio of harvest titer to bioreactor titer obtained from samples taken at similar time points was calculated to provide insight into product sieving.

3 | RESULTS

3.1 | Pressure characterization of TFF, rTFF, and HPTFF

Measurement of pressure gradients within the hollow fiber and on the filtrate side along the filter length for the TFF, rTFF, and HPTFF system was performed with a special characterization setup enabling the operation of all three systems (Figure 1a). This setup not only allowed us to measure the retentate loop and filtrate pressures at the inlet of the filter module (PT_{R1} and PT_{F1}) and at the outlet of the filter module (PT_{R2} and PT_{F2}), but enabled us to get additional measurements of the filtrate pressure along the filter module length (PT_{A1-5}). A crossflow ramping from 0 to 1500 mL/min to simulate the TFF system or one of the rTFF phases demonstrated that the axial pressure drop within the retentate loop increased with increasing crossflow as seen in the diverging retentate inlet pressure PT_{R1} and retentate outlet pressure PT_{R2} (Figure 2a). All remaining pressure sensors on the filtrate side, irrespective of the crossflow, indicated the average pressure of PT_{R1} and PT_{R2}. Aligning the pressures at a crossflow of 650 mL/min according to their position revealed positive TMP at the filter inlet and negative TMP at the filter outlet. The TMP was zero in the middle of the filtration module (Figure 2c). A similar crossflow ramping was performed to characterize pressures for the HPTFF system with activated delta pressure control to match the filtrate inlet pressure PT_{F1} with the retentate inlet pressure PT_{R1} (Figure 2b). In contrast to the TFF and rTFF, filtrate pressures along the filter were not identical anymore but matched the retentate pressure gradient along the entire filter length (Figure 2d). The only filtrate pressure sensor with a discrepancy to the respective retentate pressure was PT_{F2}. This discrepancy was negligible for crossflows below 400 mL/min but increased slightly with larger crossflow (Figure 2b). Required co-current filtrate flows for varying crossflows using the lab-scale filter are provided in the Supporting Information SI: Figure 1A.

Time-resolved pressure recordings for the operation of a TFF and rTFF system at a crossflow of 650 mL/min are provided in Figure 2e. TFF is represented by only considering the forward crossflow phase. The rTFF is described by adding a reverse crossflow phase, and thereby alternating the crossflow. The only changing pressures upon crossflow reversal were the retentate pressures, with PT_{R1} taking the

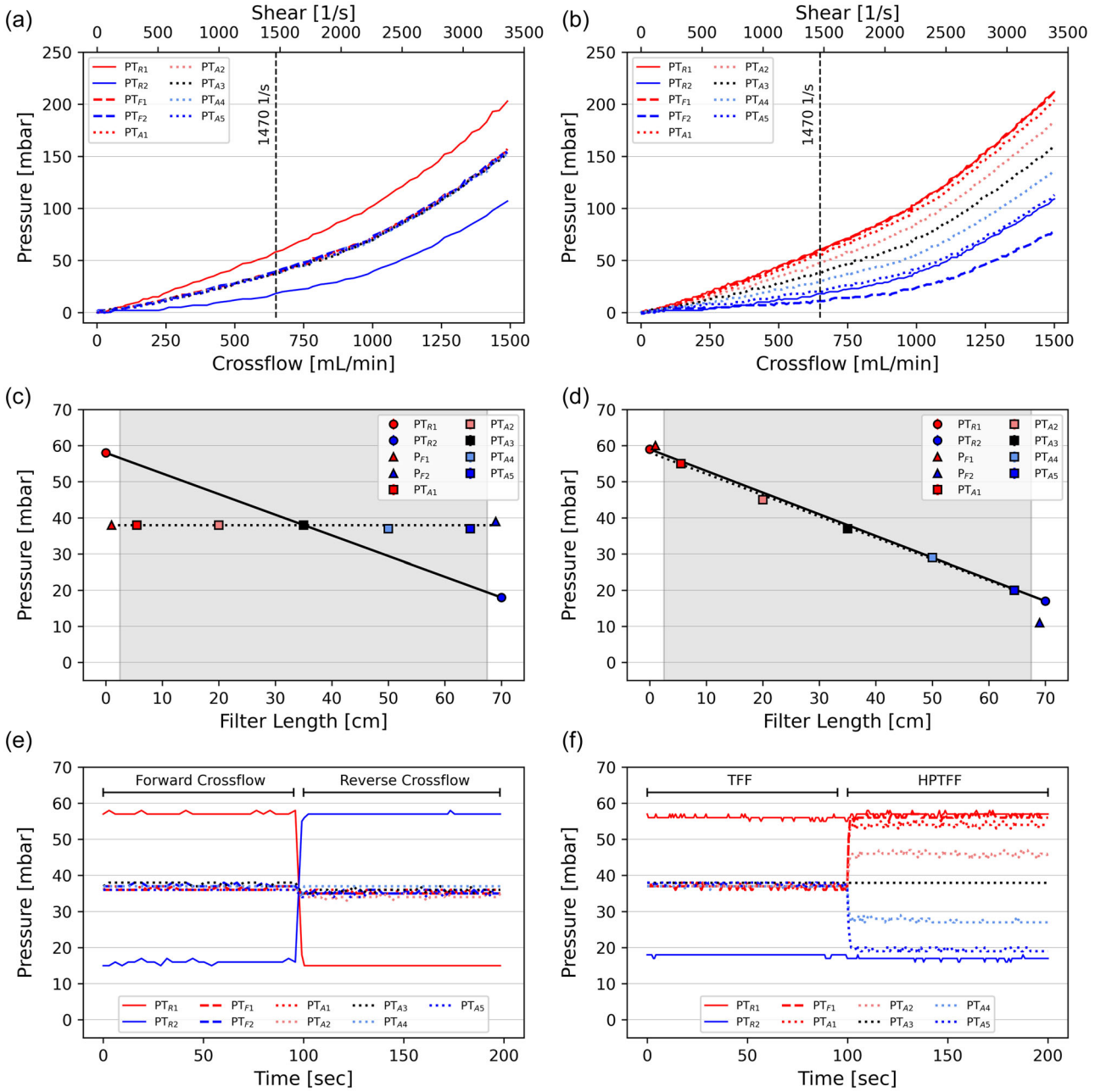

FIGURE 2 Pressure characterization results for tangential flow filtration (TFF), reverse TFF (rTFF), and high-performance TFF (HPTFF) operation using water as medium. Crossflow ramping in TFF and rTFF operation (a) and crossflow ramping with delta pressure control in HPTFF operation (b). Dashed lines represent the standard operating region of 1470 s^{-1} shear resulting in approximately 650 mL/min crossflow. Pressure measurements according to their position along the filter length are provided for TFF and the forward crossflow phase of rTFF (c), and for HPTFF (d), gray areas represent absolute fiber length. Pressure distributions at 650 mL/min crossflow versus time are shown for TFF and rTFF (e), where the forward crossflow phase corresponds to TFF operation, and rTFF is defined by alternation between forward and reverse crossflow. HPTFF pressure distribution versus time upon co-current filtrate flow activation was further measured at 650 mL/min crossflow (f).

previous value of PT_{R2} and vice-versa. HPTFF operation at 650mL/min crossflow was achieved upon delta pressure control activation with a co-current filtrate flow of approximately 1400 mL/min (Figure 2f). Immediately, filtrate pressures align with the retentate pressure gradient and are stably maintained at the target values.

A schematic representation of the pressure characterization experiments summarizes the findings for the TFF system (Figure 3a), rTFF system (Figure 3b), and for HPTFF system (Figure 3c). The schematic pressure plots demonstrate the TMP differences along the fiber length for the TFF and the rTFF system. A zoomed view into a hollow fiber at the beginning, in the middle and at the end of the filter module further highlights the Starling recirculation indicated by arrows. Compared to the TFF and rTFF system, the filtrate pressures in the HPTFF system are well aligned with the retentate pressures

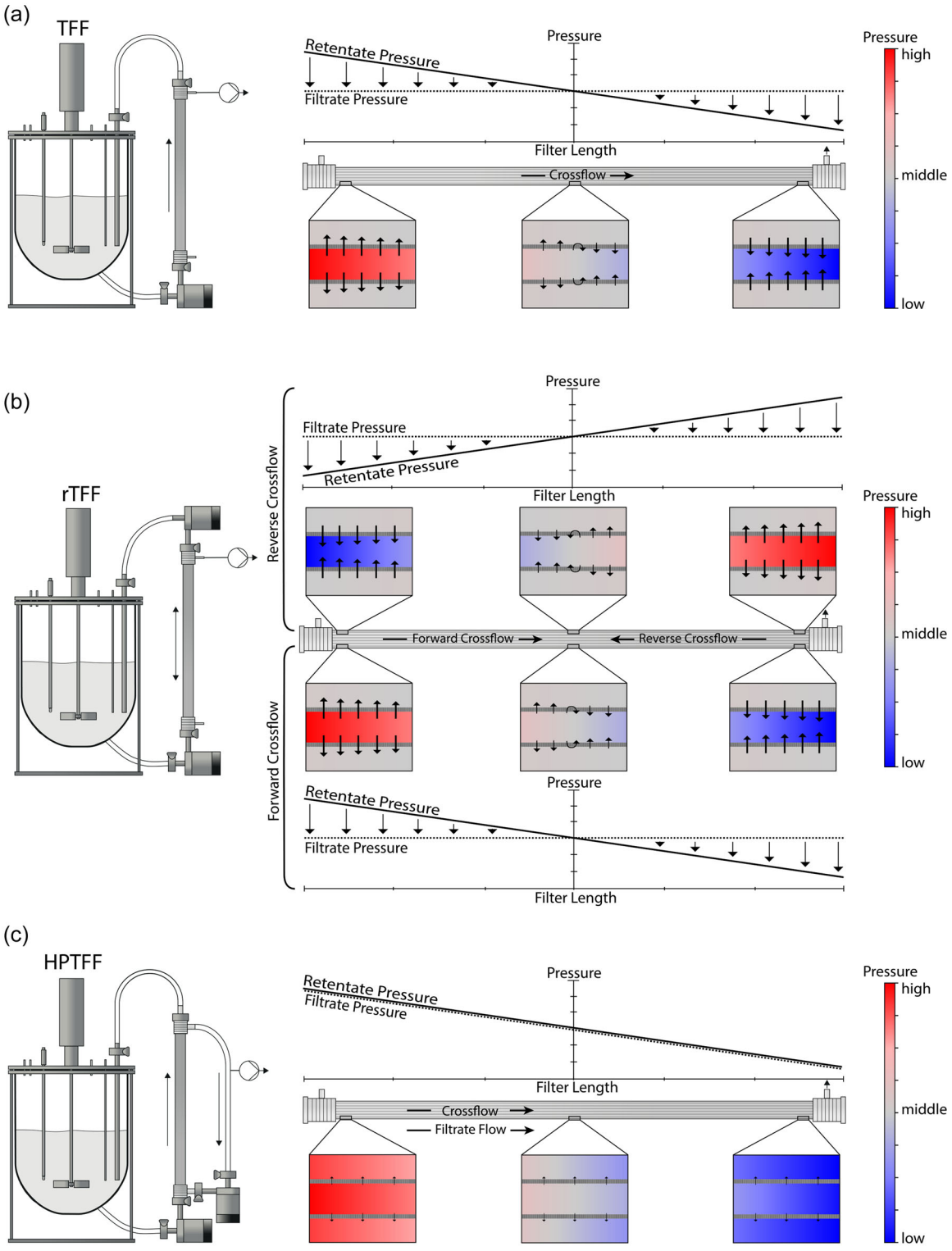

FIGURE 3 Schematic representation for tangential flow filtration (a), reverse tangential flow filtration (rTFF) (b), and high-performance TFF (c) systems with centrifugal pumps based on pressure characterization. Pressure curves along the filter length for each system are given and arrows indicate filtrate flux, longer arrows represent larger fluxes. Additionally, a zoom into a fiber at the beginning, middle, and at the end of the filter is provided and colored from red (high pressure) to blue (low pressure). As rTFF consist of two phases, the situation for forward crossflow and reverse crossflow are depicted.

thereby generating a uniform TMP of only slightly above zero along the length of the filtration module. Small arrows from retentate to filtrate indicate that the entire filtration area is utilized for filtration by avoiding Starling recirculation.

3.2 | Pressure characterization of scTFF

Whereas HPTFF operation focused on matching filtrate pressures with the retentate pressure gradient and thereby removing Starling recirculation completely, we also examined a novel operating mode for unidirectional TFF defined as scTFF. The scTFF consists of two phases, a first phase with lower co-current filtrate flow than required for HPTFF, and a second phase with higher co-current filtrate flow, resulting in a step profile for the co-current filtrate flow (Figure 4a). To demonstrate the impact of co-current filtrate flow on the pressure profiles, a co-current filtrate flow ramping was performed by fixing the retentate crossflow to 650 mL/min (Figure 4b). At 0mL/min co-current filtrate flow, the system basically corresponded to a standard TFF operation. With increasing co-current filtrate flow, the pressure aligned more and more to the retentate pressure gradient and matched it at about 1400 mL/min, corresponding to the situation in HPTFF operation. Further increasing the co-current filtrate flow led to higher filtrate pressures in the first half of the filter and lower filtrate pressures in the second half of the filter compared to the retentate pressure gradient. The filtrate pressure at the outlet PT_{F2} was not plotted as similar discrepancies to the retentate pressure gradient as seen in Figure 2b were observed. Selecting a co-current filtrate flow of 870 mL/min for phase 1 (blue vertical dashed line) and 1890 mL/min for phase 2 (red vertical dashed line) of the scTFF operation, a delta pressure between PT_{R1} and PT_{F1} of −10 and +10 mbar, respectively, was achieved. Pressures recorded for the two phases of scTFF were then plotted according to their position along the filter (Figure 4c). The black line represents the retentate pressure gradient, the blue dashed line represents the pressure drop on the filtrate side for scTFF phase 1 and the red line represents the pressure drop on the filtrate side for scTFF phase 2. A common intersection of all three lines was located in the middle of the filter length, meaning the absolute TMP is zero in the middle of the filter and gets larger the closer to one of two filter ends.

By switching between scTFF phase 1 and scTFF phase 2 with defined phase times, a scTFF system with unidirectional crossflow but reversing Starling recirculation was obtained (Figure 4c). Red areas represent the flux of filtrate back into the retentate due to higher filtrate pressures compared to the retentate pressures, whereas blue areas represent flux from retentate to filtrate due to higher retentate pressures compared to filtrate pressures. As such, filtrate pressure PT_{A1} positioned at 5.5 cm from the filter inlet was lower than the corresponding retentate pressure at 5.5 cm filter length (black dashed line) during scTFF phase 1 and got larger than the corresponding retentate pressure during scTFF phase 2. Similar, but reversed, behavior was observed for pressure PT_{A5} positioned on the second half of the filter at 64.5 cm filter length. In this case, PT_{A5} was larger than the retentate pressure during scTFF phase 1 and smaller than the retentate pressure during scTFF phase 2. A combined HPTFF-scTFF operation is also possible by integrating a sweeping into the HPTFF operation. The sweeping was achieved by lowering the co-current filtrate flow (scTFF phase 1) and subsequently increasing the co-current filtrate flow (scTFF phase 2). After the sweep, the system was again operated at HPTFF conditions (Figure 4d).

3.3 | Characterization of performance in perfusion cell culture processes

Cell culture parameters and product retention were compared for TFF, rTFF, HPTFF, and scTFF operation in steady-state perfusion processes. For all four cell retention setups (Figure 1b–d), steady-state operation was achieved after approximately 5 days and culture viability was not impacted by the cell retention operating mode (Figure 5a). Target process runtime of 30 days was achieved for all runs except TFF_1 and HPTFF_2. These runs were terminated at Day 19 (TFF_1) and Day 21 (HPTFF_2) due to a sudden decrease in crossflow caused by inlet blocking of the fibers. Cell debris increased for most runs until Day 25, after which a slight decrease in cell debris was observed. In general, TFF and rTFF runs showed slightly higher debris levels compared to HPTFF and scTFF runs especially after Day 13 (Figure 5b). The harvest titer plot (Figure 5c) and the product sieving plot (Figure 5d) revealed significantly reduced product sieving of around 80% for the TFF operation after only a few first days of steady-state operation. Product sieving further decreased down to 60% or lower for TFF. Product sieving for rTFF stayed above 90% for the entire experiment for run rTFF_1 and remained above 80% for run rTFF_2. HPTFF operation resulted in similar or even higher product sieving with yields above 95% for the entire run. Cell diameter increased slightly with runtime for all of the cell retention systems and pH stayed within the defined range of 7.07 ± 0.17 for all runs (Supporting Information SI: Figure 2A,B).

Cell culture bioreactors must be oxygenated to support cell growth by sparging air or oxygen. Centrifugal pumps in unidirectional crossflow operations (TFF, HPTFF, and scTFF) tend to accumulate gas bubbles coming into the cell recirculation loop. This problem was solved by stopping the pumps for 3 s every 3 min to release the air from the pump head. With activated delta pressure control during HPTFF operation controlling delta pressure to 0 mbar, stopping the crossflow for 3 s caused a sharp change in the pressure profile along the filter length (Figure 6a). Due to some delay of the proportional-integral controlled co-current filtrate flow regulation, the filtrate pressure PT_{F1} was higher than the retentate pressure PT_{R1} immediately after crossflow stopping, which resulted in a negative delta pressure up to −14 mbar (Figure 6b red area). After reactivation of the crossflow, the co-current filtrate flow was reduced and the proportional-integral control required some more time to establish HPTFF conditions. During that time interval, a positive delta pressure of up to 5 mbar was seen at the filter inlet (Figure 6b blue area). Taken together, stopping the crossflow during HPTFF operation

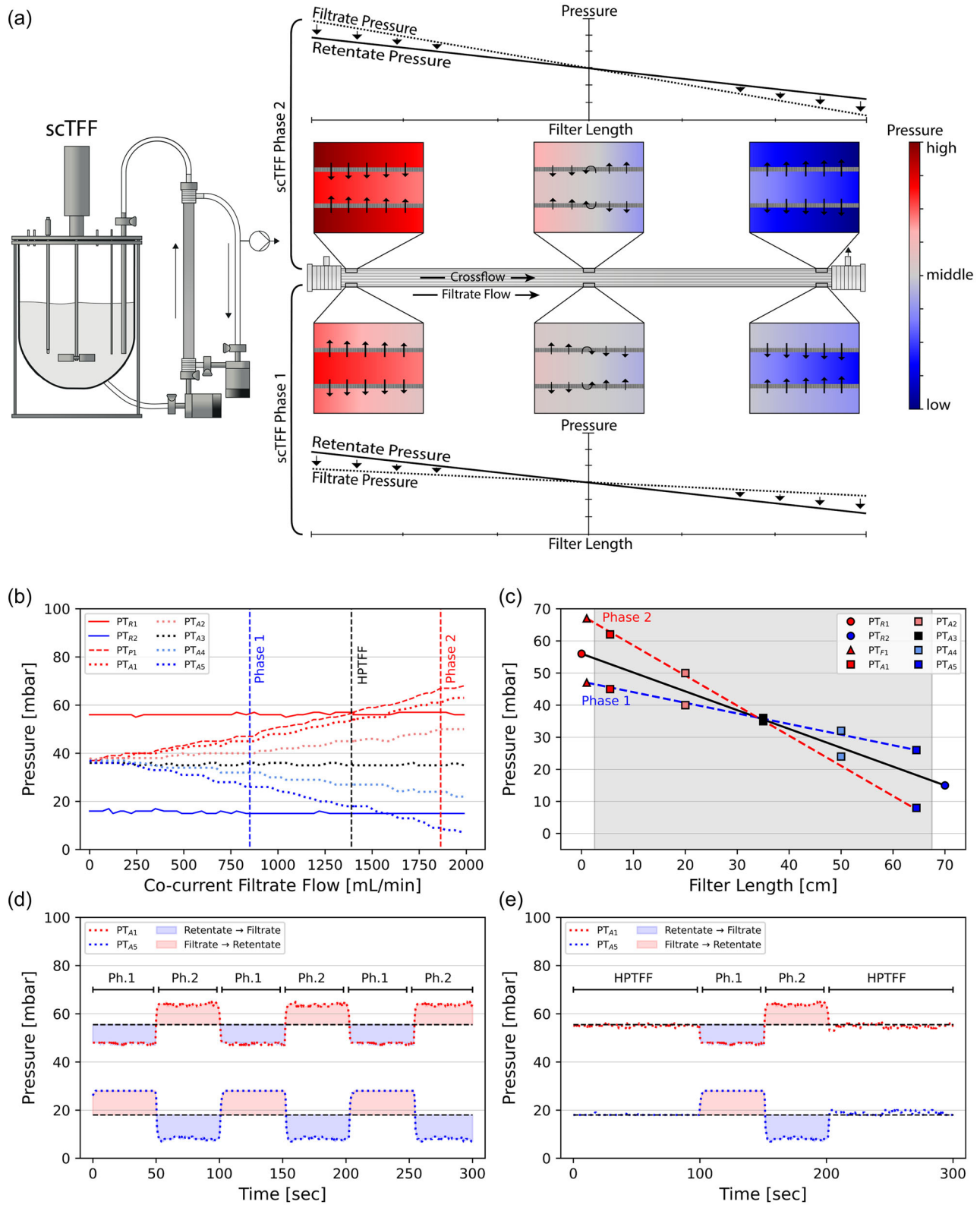

FIGURE 4 Concept of stepping co-current tangential flow filtration (scTFF) by schematic representation of pressure gradient along filter length (a). Co-current flow ramping at 650 mL/min crossflow (b). Vertical dashed lines represent operating conditions for high-performance TFF (HPTFF) (black), scTFF phase 1 with −10 mbar pressure difference (blue), and scTFF phase 2 with +10 mbar pressure difference (red) on filter inlet. Pressure measurements according to their position along the filter length are provided for all three dashed lines (c), gray areas represent absolute fiber length. Operation of scTFF with two alternating phases (±10 mbar pressure difference) is demonstrated by time-resolved pressure distribution plots (d). Alternative operating mode of HPTFF with alternating membrane sweeps by scPTFF phases of ±10 mbar in between HPTFF phases (e). Red areas represent flux of filtrate back into the retentate, blue areas represent flux from retentate to filtrate. Water as a medium was used for all pressure tests.

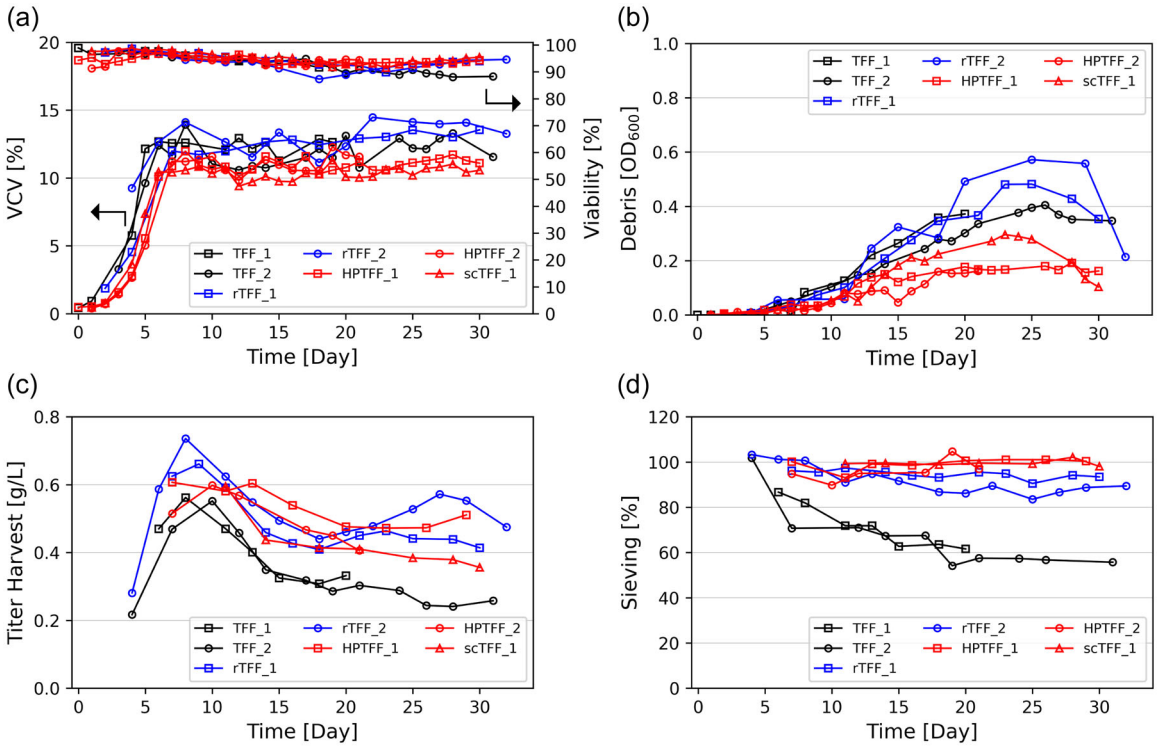

FIGURE 5 Perfusion cell culture runs with tangential flow filtration (TTF) (black), reverse TTF (blue), high-performance TFF, or stepping co-current TFF (red) as cell retention devices. Viable cell volume and viability (a), cell culture debris (b), harvest titer (c), and product sieving (d).

resulted in a slight membrane sweeping. In rTFF operation, gas bubble trapping was alleviated by positioning the pumps such that they are pointing toward each other, with air removed from the pump head by alternating activation of the retentate pumps.

3.4 | Large-scale filter pressure characterization

Large-scale experiments using TFF, HPTFF, and scTFF operation confirmed results from the lab-scale experiments. Crossflow ramping from 0 to 45 L/min showed a continued increase in the pressure gradient along the filter length in TFF operation while the permeate pressures were independent of position (Figure 7c). Considering similar crossflow conditions with 29 L/min corresponding to a shear rate of 1470 s^{-1} as applied during lab-scale perfusion cell culture runs resulted in a fiber inlet pressure of 71 mbar (PT_{RC1}), a fiber outlet pressure of 31 mbar (PT_{RC2}) and an average filtrate pressure (PT_{A1-5}) of 51 mbar (Figure 7e). Filtrate pressures on the filtrate inlet and outlet side (PT_{A1-5}) showed similar values as the filtrate pressure sensors on the backside of the filter module (PT_{AB1-5}).

HPTFF operation could be achieved by controlling pressure PT_{F1} so that it was 6 mbar above the pressure PT_{R1} for all evaluated crossflows up to 45 L/min (Figure 7d). Filtrate pressures on the filtrate inlet and outlet side (PT_{A1-5}) were aligned with the corresponding filtrate pressures on the backside (PT_{AB1-5}) (Figure 7f). In contrast to TFF operation, filtrate pressures matched the pressure gradient of the retentate loop, with pressure sensors PT_{A1} and PT_{AB1} slightly lower than the corresponding retentate pressures. The filtrate outlet pressure PT_{F2} was significantly lower compared to the other pressure sensor readings. Co-current filtrate flows to achieve HPTFF at varying crossflows are provided in the Supporting Information SI: Figure 1B.

scTFF operation to generate controlled Starling recirculation was further demonstrated with a large-scale filter module and the data are provided in the Supporting Information SI: Figure 3. As such, a filtrate loop ramping at constant crossflow (Supporting Information SI: Figure 3A) and pressure distribution along the filter length for scTFF phase 1 (Supporting Information SI: Figure 3B) and for scTFF phase 2 (Supporting Information SI: Figure 3C) are provided. In addition to changing the filtrate flow, a crossflow stop whilst keeping the filtrate proportional-integral control active was able to achieve effective membrane sweeping (Supporting Information SI: Figure 3D).

4 | DISCUSSION

Applying co-current filtrate flow represents a promising tool to alleviate product retention in mammalian perfusion processes by achieving uniform TMP conditions along the filter length. This decreases (or eliminates) the Starling recirculation flow, reducing the filter load by using the entire membrane surface (Radoniqi et al., 2018). In this study, pressure characterization experiments demonstrated that HPTFF operation is possible for a wide range of

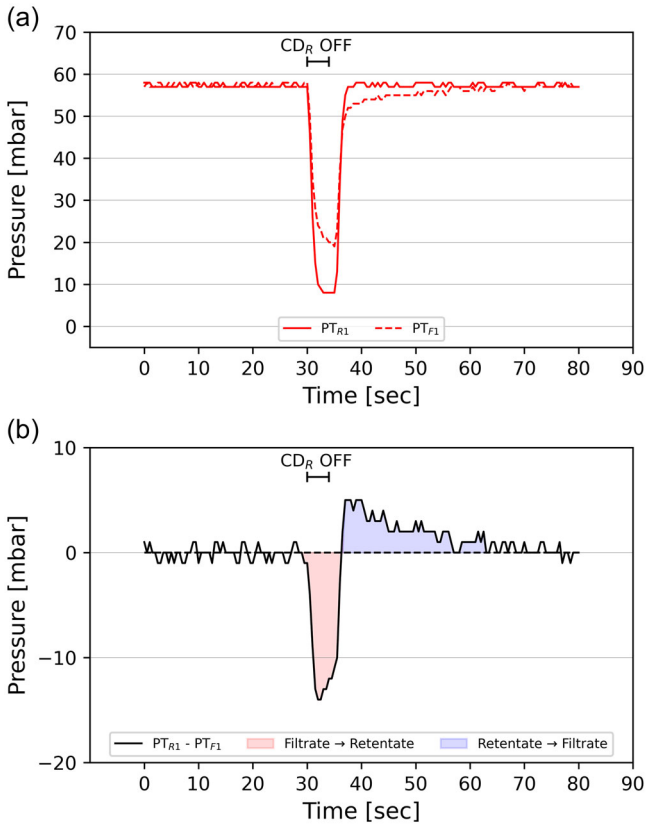

FIGURE 6 Membrane sweep in high-performance tangential flow filtration (HPTFF) operation upon crossflow stop. Inlet pressure of the retentate (PT_{R1}) and inlet pressure on filtrate side (PT_{F1}) were recorded upon a 3 s stop of the levitated centrifugal pump (CD_{R1}) to release air bubbles (a). The delta pressure ($PT_{R1} - PT_{F1}$) was calculated and the blue area represents a negative delta pressure during which a backflush is happening in the first half of the filter, whereas the red area represents a positive delta pressure resulting in a backflush at the second half of the filter (b).

perfusion-relevant crossflows using levitated centrifugal pumps that provide uniform (nonpulsatile) flow (Figure 2b). By matching the inlet retentate pressure PT_{R1} and the inlet filtrate pressure PT_{F1} with a simple delta pressure control to 0 mbar, a uniform TMP was achieved along the entire length of the lab-scale filter (Figure 2c). Interestingly, the outlet filtrate pressure PT_{F2} showed increasing discrepancy from the retentate outlet pressure (PT_{R2}) with increasing co-current filtrate flow. This discrepancy may come from increasing turbulence at the filtrate outlet, although it had no effect on the filtrate pressure profile (PT_{A1-5}). A reduced setup consisting of two pressure sensors (PT_{R1} and PT_{F1}), a retentate centrifugal pump (CD_{R1}), and a filtrate centrifugal pump (CD_F) are, therefore, sufficient to operate the HPTFF system (Figure 1d).

Large-scale pressure characterization revealed that HPTFF can also be achieved with manufacturing scale filters (Figure 7). With the filtration module used in this study, the inlet filtrate pressure PT_{F1} had to be increased by 6 mbar compared to the inlet retentate pressure PT_{R1} to match the filtrate pressures PT_{A1-5} with the retentate pressure drop. A pressure decrease from PT_{R1} positioned in the inlet retentate tubing compared to the pressure sensor located in the adapter piece connecting tube was observed (Figure 7d,f). This offset might be due to the change in tube diameter from the inlet tubing to the much wider adapter piece connecting to the hollow fiber module. Further, pressure PT_{F1} had to be controlled higher than expected to achieve HPTFF. As already observed in lab-scale, the outlet pressure sensor in the filtrate loop PT_{F2} was lower than anticipated. These findings might be explained by a combination of a relatively smaller filtrate inlet adapter diameter than in the lab-scale and perturbation of the flow pattern at elevated co-current filtrate flows in the large-scale module. Nevertheless, the determination of the offset by pressure characterization allowed us to achieve HPTFF operation across the entire tested crossflow range from 0 to 45 L/min by only measuring pressures PT_{R1} and PT_{F1}. Additionally, PT_{AB1-5}, positioned on the opposite side where filtrate enters and leaves the hollow fiber module, was in good agreement with the pressure sensors located on the side where the filtrate inlet and outlet are located (PT_{A1-5}). This demonstrates that radial pressure is equally distributed in the large filtration modules and the filtrate inlet and outlet do not influence the pressure profile.

In perfusion cell culture, a uniform TMP, as per definition in HPTFF, is not necessarily the highest priority as in protein separations (van Reis, 1993; van Reis et al., 1997). The main objective in perfusion processes is to avoid filter clogging and reduce product retention. Therefore, a membrane sweep from time to time in the form of a backflush can be beneficial to remove some deposited material, but avoiding intense backflushing as attributed to irreversible fouling (Weinberger & Kulozik, 2022). A novel operating mode was designed in this study named scTFF. scTFF can be operated with the same hardware setup as described for the HPTFF (Figure 1d). By lowering and subsequently increasing the co-current filtrate flow rate compared to HPTFF operation, a TMP gradient was achieved along the filter length resulting in a Starling recirculation (Figure 4a). The Starling recirculation changed direction upon switching from scTFF phase 1 to 2, generating a backflush on the first half of the filter and then on the second half of the filter similar to what occurs in ATF or rTFF operation (Pappenreiter et al., 2023; Radoniqi et al., 2018; Weinberger & Kulozik, 2022). In contrast to ATF and rTFF, where the strength of the Starling recirculation is a function of crossflow velocity and filter length, the strength of the Starling recirculation in scTFF can be tuned independently of both crossflow velocity and fiber length. For demonstration, a TMP of ±10 mbar was targeted (Figure 4c), but any other TMP larger or smaller can be achieved just by varying the co-current filtrate flow rates (Figure 4b). Furthermore, scTFF can either be operated by switching between scTFF phases 1 and 2 (Figure 4d), or by operating at HPTFF conditions and integrating a membrane sweeping from time to time by lowering or increasing the co-current filtrate flow (Figure 4e). The duration of each phase can thereby freely be chosen, giving even more operational flexibility. scTFF operation was demonstrated at lab-scale, and pressure characterization experiments revealed applicability at the manufacturing scale without changing the system setup (Supporting Information SI: Figure 3).

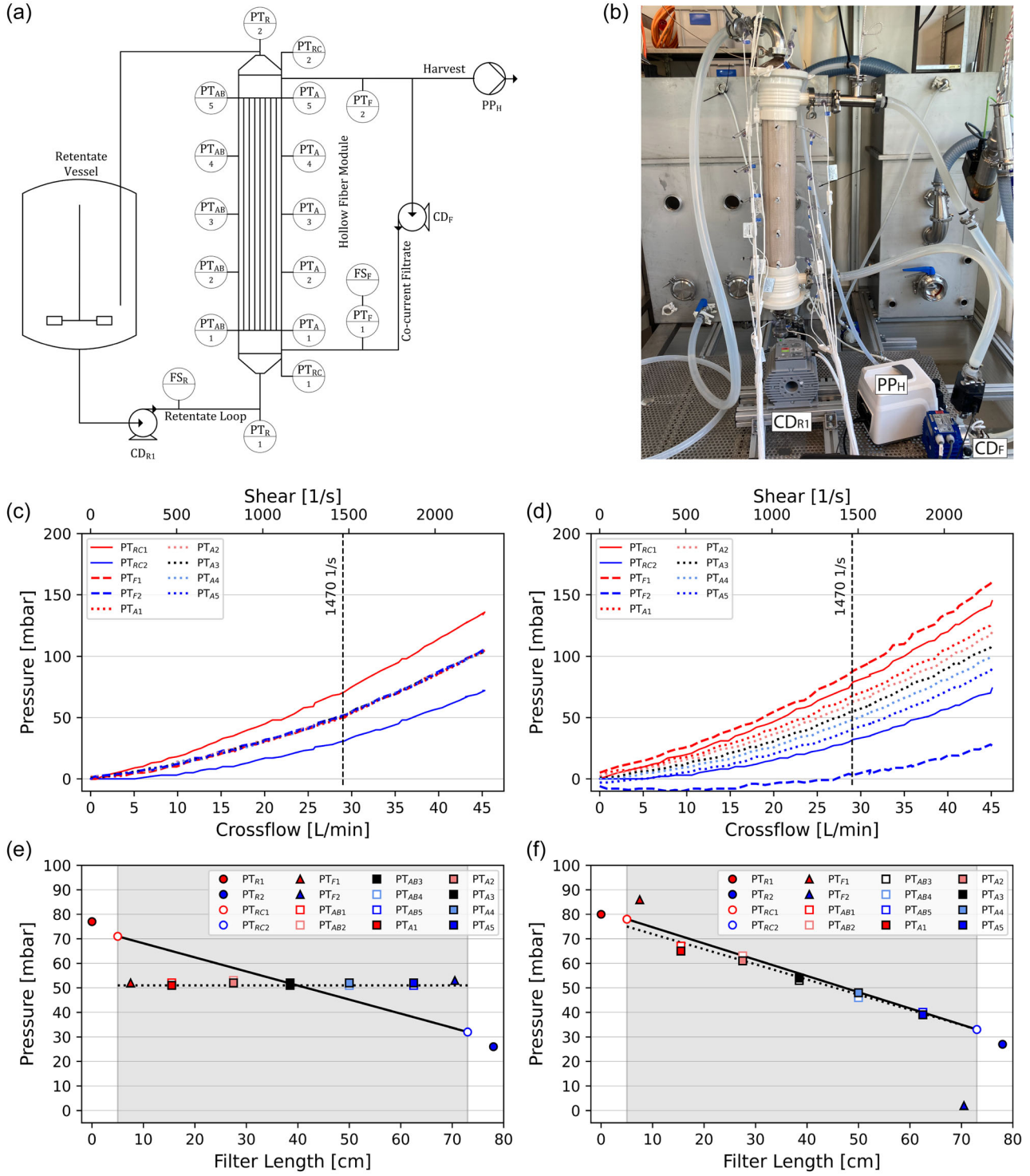

FIGURE 7 Large-scale pressure characterization results using water as a medium. Schematic representation of the experimental setup for the large-scale pressure characterization (a). Pressure transmitters (PT), flow sensors (FS), centrifugal pumps (CD) and peristaltic pumps (PP) are specified with subscripted letters according to their position (A and AB, additional sensors on filtrate side; F, filtrate; H, harvest; R, retentate). Picture of experimental setup (b). Large-scale crossflow ramping in tangential flow filtration (TFF) operation (c) and crossflow ramping with delta pressure control in high-performance TFF (HPTFF) operation (d). Pressure measurements according to their position along the filter length are provided for TFF (e) and for HPTFF (f) at standard operation of 1470 s^{-1} shear, gray areas represent absolute fiber length.

Perfusion cell culture runs revealed significantly reduced product sieving below 60% for TFF operation (Figure 5d). This agrees with the literature, where similarly reduced product sieving was reported (Karst et al., 2016; Pappenreiter et al., 2023; Wang et al., 2017). While filtrate flux in ATF systems typically ranges from 2 to 3 L/m^2/h (Radoniqi et al., 2018; Romann et al., 2023), previous studies have shown that operation at filtrate flux below 1 L/m^2/h caused less fouling and product retention (Walther et al., 2019). Even with the low filtrate flux of 0.6 L/m^2/h selected in this study to minimize fouling, significant differences in product sieving depending on the operating mode were observed. Despite similar pressure drop and, therefore, comparable absolute Starling recirculation flow of rTFF compared to TFF, rTFF showed significantly improved product sieving above 90%, which is comparable to what has been observed in ATF systems (Pappenreiter et al., 2023). This confirms that with an identical pump system, rTFF clearly outperformed TFF. However, this study does not allow us to distinguish between the beneficial contributions of backflushing at both the inlet and outlet, utilization of the entire membrane surface, and/or relaxation of the fouling deposit when the crossflow direction changes. The rTFF_2 run with higher amount of cell culture debris showed lower product sieving than rTFF_1 (Figure 5d), highlighting that rTFF is still prone to product retention which can likely be attributed to pronounced fouling at the inlet or exit of the hollow fiber modules at elevated debris levels (Sundar et al., 2023).

HPTFF operation entirely removing Starling recirculation due to a uniform TMP along the filtration module showed similar or even higher product sieving than rTFF operation. The HPTFF operation was interrupted every 3 min for 3 s by stopping the crossflow to release potentially trapped gas bubbles from the centrifugal pump head, which might even have had a beneficial impact on product sieving. The slightly delayed proportional-integral response controlling the co-current filtrate flow resulted in a quick sweep of the membrane, initially backflushing the membrane in the first filter half, followed by backflushing of the second filter half upon crossflow reactivation (Figure 6). Whereas bubble trapping in the centrifugal pump head plays a minor role at larger scales, intentional pump stopping from time to time to generate a membrane sweep in HPTFF operation might still be an attractive option (Supporting Information SI: Figure 3D). It must be mentioned that a similar effect can be achieved by shortly increasing the crossflow by maintaining the co-current filtrate flow proportional-integral control active.

Similar but more controlled sweeping of the membrane was alternatively achieved by increasing or lowering the co-current filtrate flow at constant crossflow (Figure 4a). Intensity and location of the backflush can be adjusted by changing the magnitude of the co-current filtrate flow (Figure 4b), offering a wide range of possibilities not available in ATF or rTFF operation. scTFF allows the Starling recirculation flow to be adjusted independently of filtration module specifications or crossflow velocities without changing the hardware setup. This novel approach enables further research to evaluate the benefits of membrane sweeping in a controlled but flexible manner to define best operating conditions depending on process requirements. This would include studies of scTFF and HPTFF operation at higher filtrate flux where membrane fouling and product retention are likely to be even more problematic.

A critical aspect of unidirectional crossflow systems remains filter inlet blocking (Weinberger & Kulozik, 2021a; Zydney, 2016). Cell clumps or aggregates getting into the cell recirculation loop can be trapped at the filter inlet blocking entire hollow fibers. In two unidirectional crossflow runs (TFF_1 and HPTFF_2) filter inlet blocking led to premature run termination. When working with cell lines prone to aggregation, rTFF should be the chosen cell retention operation mode to prevent inlet blocking by crossflow reversal, else, filters must be exchanged to maintain high filtration performance. When aggregation is not an issue and unidirectional crossflow represents no risk to premature run termination, HPTFF or scTFF clearly outperform conventional TFF operation. Further, HPTFF and scTFF offer greater flexibility compared to ATF or rTFF systems by alleviating previously described restrictions on filter characteristics and operation parameters:

(1) Crossflow velocity: No restriction to low crossflows as strategy to avoid extensive Starling recirculation.
(2) Filtration module length: Enabling longer filtration modules due to TMP control and thereby reducing system complexity with multiple parallel modules.
(3) Inner fiber diameter: No need for increased inner fiber diameters to reduce pressure gradient at the cost of membrane surface area or greater hold-up volume.
(4) Pore size: Possibility to utilize larger pores sizes without increasing Starling recirculation caused by lower membrane resistance.

5 | CONCLUSION

This study evaluated the impact of co-current filtrate flow on product retention during steady-state perfusion processes using hollow fiber modules as cell retention devices. Whereas Starling recirculation in TFF and alternating crossflow TFF is dependent on crossflow velocity and filter module characteristics, co-current filtrate flow enabled independent control of Starling recirculation. Pressure characterization studies performed by inserting additional pressure sensors along the filter module length revealed detailed insights into the filtrate pressure gradient and confirmed the theoretical concept of altering TMP by co-current filtrate flow. Further, control of Starling flow was not only demonstrated at lab-scale, but also successfully applied to a manufacturing scale filtration module. The benefits of HPTFF operation or precisely controlling the direction and intensity of Starling recirculation in scTFF operation was further demonstrated in steady-state perfusion cell culture processes which showed much higher product sieving compared to standard TFF operation. Starling flow control enabled by co-current filtrate flow operation represents an effective tool not only to study filter fouling but also to reduce product retention in steady-perfusion cell culture processes as well as other operations such as dynamic perfusion or N-1 perfusion.

AUTHOR CONTRIBUTIONS

Patrick Romann: Conceptualization, formal analysis, investigation, methodology, visualization, writing—original draft. **Philip Giller**: Data curation, formal analysis, investigation, methodology. **Christoph Herwig**: Conceptualization, methodology, supervision, writing—review and editing. **Andrew L. Zydney**: Conceptualization, methodology, supervision, writing—review and editing. **Arnaud Perilleux**: Resources, supervision, writing—review and editing. **Jonathan Souquet**: Resources, supervision, writing—review and editing. **Jean-Marc Bielser**: Conceptualization, investigation, project administration, resources, supervision, visualization, writing—review and editing. **Thomas K. Villiger**: Conceptualization, investigation, project administration, resources, supervision, visualization, writing—review and editing.

ACKNOWLEDGMENTS

The authors would like to thank Pavel Dagorov and his workshop team (FHNW) for hollow fiber filter modification and Sebastian Schneider and Silvia Pavone (FHNW) for supporting experimental work on perfusion processes. The authors also thank the entire Levitronix team for support, especially Philipp Campos, Lorenz Schüssler, and Knut Kuss for valuable inputs and support. Dominik Schieman, Paul Niepold, and David Garcia Munzer (Novartis) kindly sponsored the manufacturing scale filter module. Moreover, the authors would like to acknowledge specifically the Bioprocess Sciences (BPS) team of Merck Serono SA (an affiliate of Merck KGaA) for material and analytical support and for valuable discussions and support throughout the project, especially Alexandre Châtelin and the analytical team.

CONFLICT OF INTEREST STATEMENT

Antony Sibilia is an employee of Levitronix GmbH, a company that produces and markets centrifugal pumps and flow sensors used in the present study. He was not involved in the interpretation of data or statistical analysis. The remaining authors declare no conflict of interest.

DATA AVAILABILITY STATEMENT

The data that support the findings of this study are available from the corresponding author upon reasonable request.

ORCID

Patrick Romann http://orcid.org/0000-0002-7555-0598
Christoph Herwig http://orcid.org/0000-0003-2314-1458
Andrew L. Zydney https://orcid.org/0000-0003-1865-9156
Jean-Marc Bielser http://orcid.org/0000-0002-9931-5920
Thomas K. Villiger http://orcid.org/0000-0003-0036-2522

REFERENCES

Belfort, G., Davis, R. H., & Zydney, A. L. (1994). The behavior of suspensions and macromolecular solutions in crossflow microfiltration. *Journal of Membrane Science*, *96*, 1–58.

Bielser, J. M., Wolf, M., Souquet, J., Broly, H., & Morbidelli, M. (2018). Perfusion mammalian cell culture for recombinant protein manufacturing—A critical review. *Biotechnology Advances*, *36*(4), 1328–1340. https://doi.org/10.1016/j.biotechadv.2018.04.011

Blaschczok, K., Kaiser, S. C., Löffelholz, C., Imseng, N., Burkart, J., Bösch, P., Dornfeld, W., Eibl, R., & Eibl, D. (2013). Investigations on mechanical stress caused to CHO suspension cells by standard and single-use pumps. *Chemie Ingenieur Technik*, *85*(1–2), 144–152. https://doi.org/10.1002/cite.201200135

Chew, J. W., Kilduff, J., & Belfort, G. (2020). The behavior of suspensions and macromolecular solutions in crossflow microfiltration: An update. *Journal of Membrane Science*, *601*(October 2019), 117865. https://doi.org/10.1016/j.memsci.2020.117865

Clincke, M. F., Mölleryd, C., Samani, P. K., Lindskog, E., Fäldt, E., Walsh, K., & Chotteau, V. (2013). Very high density of Chinese hamster ovary cells in perfusion by alternating tangential flow or tangential flow filtration in WAVE bioreactor™—Part II: Applications for antibody production and cryopreservation. *Biotechnology Progress*, *29*(3), 768–777. https://doi.org/10.1002/btpr.1703

Coffman, J., Brower, M., Connell-Crowley, L., Deldari, S., Farid, S. S., Horowski, B., Patil, U., Pollard, D., Qadan, M., Rose, S., Schaefer, E., & Shultz, J. (2021). A common framework for integrated and continuous biomanufacturing. *Biotechnology and Bioengineering*, *118*(4), 1721–1749. https://doi.org/10.1002/bit.27690

Field, R. (2010). Fundamentals of fouling. In K.-V. Peinemann, & S. P. Nunes (Eds.), *Membrane technology* (Vol. 44, pp. 1–23). Wiley-VCH Verlag GmbH & Co. KgaA. https://doi.org/10.1002/9783527631407.ch1

Fisher, A. C., Kamga, M.-H., Agarabi, C., Brorson, K., Lee, S. L., & Yoon, S. (2019). The current scientific and regulatory landscape in advancing integrated continuous biopharmaceutical manufacturing. *Trends in Biotechnology*, *37*(3), 253–267. https://doi.org/10.1016/j.tibtech.2018.08.008

Grzenia, D. L., Carlson, J. O., & Wickramasinghe, S. R. (2008). Tangential flow filtration for virus purification. *Journal of Membrane Science*, *321*(2), 373–380. https://doi.org/10.1016/j.memsci.2008.05.020

Karst, D. J., Serra, E., Villiger, T. K., Soos, M., & Morbidelli, M. (2016). Characterization and comparison of ATF and TFF in stirred bioreactors for continuous mammalian cell culture processes. *Biochemical Engineering Journal*, *110*, 17–26. https://doi.org/10.1016/j.bej.2016.02.003

Kelly, W., Scully, J., Zhang, D., Feng, G., Lavengood, M., Condon, J., Knighton, J., & Bhatia, R. (2014). Understanding and modeling alternating tangential flow filtration for perfusion cell culture. *Biotechnology Progress*, *30*(6), 1291–1300. https://doi.org/10.1002/btpr.1953

Kim, S. C., An, S., Kim, H. K., Park, B. S., Na, K. H., & Kim, B. G. (2016). Effect of transmembrane pressure on factor VIII yield in ATF perfusion culture for the production of recombinant human factor VIII co-expressed with von Willebrand factor. *Cytotechnology*, *68*(5), 1687–1696. https://doi.org/10.1007/s10616-015-9918-1

MacDonald, M. A., Nöbel, M., Roche Recinos, D., Martínez, V. S., Schulz, B. L., Howard, C. B., Baker, K., Shave, E., Lee, Y. Y., Marcellin, E., Mahler, S., Nielsen, L. K., & Munro, T. (2022). Perfusion culture of Chinese Hamster Ovary cells for bioprocessing applications. *Critical Reviews in Biotechnology*, *42*(7), 1099–1115. https://doi.org/10.1080/07388551.2021.1998821

Matanguihan, C., & Wu, P. (2022). Upstream continuous processing: recent advances in production of biopharmaceuticals and challenges in manufacturing. *Current Opinion in Biotechnology*, *78*, 102828. https://doi.org/10.1016/j.copbio.2022.102828

Merin, U., & Daufin, G. (1990). Crossflow microfiltration in the dairy industry: state-of-the-art. *Le Lait*, *70*(4), 281–291. https://doi.org/10.1051/lait:1990421

Metze, S., Ruhl, S., Greller, G., Grimm, C., & Scholz, J. (2020). Monitoring online biomass with a capacitance sensor during scale-up of industrially relevant CHO cell culture fed-batch processes in single-use bioreactors. *Bioprocess and Biosystems Engineering*, *43*(2), 193–205. https://doi.org/10.1007/s00449-019-02216-4

Pappenreiter, M., Schwarz, H., Sissolak, B., & Jungbauer, A. (2023). Product sieving of mab and its high molecular weight species in different modes of ATF and TFF perfusion cell cultures. *Journal of Chemical Technology & Biotechnology*, *98*, 1658–1672. https://doi.org/10.1002/jctb.7386

Pavlik, R. (2017). *United States Patent* (Patent No. US 2019/0201820 A1).

Pavlik, R. (2019). *Australian Patent* (Patent No. W O 2019/133487 A1).

Radoniqi, F., Zhang, H., Bardliving, C. L., Shamlou, P., & Coffman, J. (2018). Computational fluid dynamic modeling of alternating tangential flow filtration for perfusion cell culture. *Biotechnology and Bioengineering*, *115*(11), 2751–2759. https://doi.org/10.1002/bit.26813

Redkar, S. G., & Davis, R. H. (1993). Crossflow microfiltration of yeast suspensions in tubular filters. *Biotechnology Progress*, *9*(6), 625–634. https://doi.org/10.1021/bp00024a009

van Reis, R. (1993). *United States Patent* (Patent No. 5,256,294).

van Reis, R., Gadam, S., Frautschy, L. N., Orlando, S., Goodrich, E. M., Saksena, S., Kuriyel, R., Simpson, C. M., Pearl, S., & Zydney, A. L. (1997). High performance tangential flow filtration. *Biotechnology and Bioengineering*, *56*(1), 71–82. https://doi.org/10.1002/(SICI)1097-0290(19971005)56:1<71::AID-BIT8>3.0.CO;2-S

van Reis, R., & Zydney, A. (2007). Bioprocess membrane technology. *Journal of Membrane Science*, *297*(1–2), 16–50. https://doi.org/10.1016/j.memsci.2007.02.045

Ripperger, S., & Altmann, J. (2002). Crossflow microfiltration—State of the art. *Separation and Purification Technology*, *26*(1), 19–31. https://doi.org/10.1016/S1383-5866(01)00113-7

Romann, P., Kolar, J., Chappuis, L., Herwig, C., Villiger, T. K., & Bielser, J.-M. (2023). Maximizing yield of perfusion cell culture processes: Evaluation and scale-up of continuous bleed recycling. *Biochemical Engineering Journal*, *193*(February), 108873. https://doi.org/10.1016/j.bej.2023.108873

Sandblom, R. M. (1978). *United States Patent* (Patent No. 4,105,547).

Shevitz, J. (2018). *United States Patent* (Patent No. US 2018/0236407 A1).

Starling, E. H. (1896). On the absorption of fluids from the connective tissue spaces. *The Journal of Physiology*, *19*(4), 312–326. https://doi.org/10.1113/jphysiol.1896.sp000596

Sundar, V., Zhang, D., Qian, X., Wickramasinghe, S. R., Smelko, J. P., Carbrello, C., Jabbour Al Maalouf, Y., & Zydney, A. L. (2023). Use of scanning electron microscopy and energy dispersive X-ray spectroscopy to identify key fouling species during alternating tangential filtration. *Biotechnology Progress*, *39*, 1–6. https://doi.org/10.1002/btpr.3336

Taddei, C., Aimar, P., Howell, J. A., & Scott, J. A. (1990). Yeast cell harvesting from cider using microfiltration. *Journal of Chemical Technology & Biotechnology*, *47*(4), 365–376. https://doi.org/10.1002/jctb.280470407

Tanaka, T., Tsuneyoshi, S. I., Kitazawa, W., & Nakanishi, K. (1997). Characteristics in crossflow filtration using different yeast suspensions. *Separation Science and Technology*, *32*(11), 1885–1898. https://doi.org/10.1080/01496399708000743

Vadi, P. K., & Rizvi, S. S. H. (2001). Experimental evaluation of a uniform transmembrane pressure crossflow microfiltration unit for the concentration of micellar casein from skim milk. *Journal of Membrane Science*, *189*(1), 69–82. https://doi.org/10.1016/S0376-7388(01)00396-9

Walther, J., McLarty, J., & Johnson, T. (2019). The effects of alternating tangential flow (ATF) residence time, hydrodynamic stress, and filtration flux on high-density perfusion cell culture. *Biotechnology and Bioengineering*, *116*(2), 320–332. https://doi.org/10.1002/bit.26811

Wang, S., Godfrey, S., Ravikrishnan, J., Lin, H., Vogel, J., & Coffman, J. (2017). Shear contributions to cell culture performance and product recovery in ATF and TFF perfusion systems. *Journal of Biotechnology*, *246* (November), 52–60. https://doi.org/10.1016/j.jbiotec.2017.01.020

Weinberger, M. E., & Kulozik, U. (2021a). On the effect of flow reversal during crossflow microfiltration of a cell and protein mixture. *Food and Bioproducts Processing*, *129*, 24–33. https://doi.org/10.1016/j.fbp.2021.07.001

Weinberger, M. E., & Kulozik, U. (2021b). Pulsatile crossflow improves microfiltration fractionation of cells and proteins. *Journal of Membrane Science*, *629*(March), 119295. https://doi.org/10.1016/j.memsci.2021.119295

Weinberger, M. E., & Kulozik, U. (2022). Understanding the fouling mitigation mechanisms of alternating crossflow during cell-protein fractionation by microfiltration. *Food and Bioproducts Processing*, *131*, 136–143. https://doi.org/10.1016/j.fbp.2021.11.003

Wolf, M., Bielser, J., & Morbidelli, M. (2020). *Perfusion cell culture processes for biopharmaceuticals*. Cambridge University Press.

Zydney, A. L. (2016). Continuous downstream processing for high value biological products: A review. *Biotechnology and Bioengineering*, *113*(3), 465–475. https://doi.org/10.1002/bit.25695

SUPPORTING INFORMATION

Additional supporting information can be found online in the Supporting Information section at the end of this article.

How to cite this article: Romann, P., Giller, P., Sibilia, A., Herwig, C., Zydney, A. L., Perilleux, A., Souquet, J., Bielser, J.-M., & Villiger, T. K. (2024). Co-current filtrate flow in TFF perfusion processes: Decoupling transmembrane pressure from crossflow to improve product sieving. *Biotechnology and Bioengineering*, *121*, 640–654. https://doi.org/10.1002/bit.28589